

## LETTERS TO NATURE

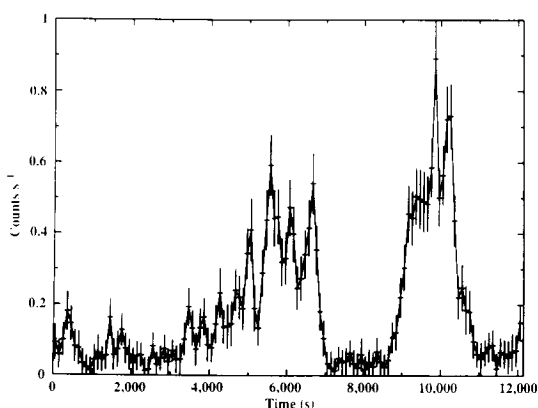


FIG. 3 The light curve of the off-axis source, folded on a 12,142-s period. A structure similar to that seen in the Ginga data<sup>3,20</sup> is apparent.

size-scales of a Galactic source. The strong and rapidly variable iron  $K\alpha$  emission line seen in the Ginga data<sup>16,17</sup> was cited as another piece of evidence in support of a supermassive black hole in NGC6814. Its strength and variability, thought to arise from the X-ray illuminated accretion flow in the active nucleus, required a substantial amount of ionized material close to the black hole<sup>17</sup>. This produces a line at 6.7 keV, so a strong gravitational redshift was required<sup>16,17</sup> in order to be consistent with the observed line energy of  $\sim 6.4$  keV. Large and variable emission lines from ionized material, however, are common in AM Her objects<sup>22</sup> and the apparent discrepancy of the line energy likely arises from the large distortion induced in the Ginga spectrum because the source is so far off axis.

Even though our result eliminates an important piece of observational evidence for black holes as the central engine in active galactic nuclei, we stress that the small central source sizes inferred from the X-ray variability of Seyfert galaxies as a class are unaffected by this finding. These sources often exhibit non-periodic, large-amplitude variability on time scales of thousands of seconds<sup>23</sup>, and the removal of NGC6814 does not substantially change the strong support that the rapid X-ray variability provides for the black hole model of active galactic nuclei<sup>24</sup>.

*Note added in proof:* After submitting this manuscript, we optically identified the periodic (off-axis) source with a 16 mag variable star, exhibiting strong He II 4,686 line emission<sup>25</sup>. The spectra also show phase-dependent, broad-emission features which we associate with cyclotron emission, thus confirming our suggestion that the source is a magnetic CV system.  $\square$

Received 20 July; accepted 31 August 1993.

1. Mittaz, J. P. D. & Branduardi-Raymont, G. *Mon. Not. R. astr. Soc.* **238**, 1029–1046 (1989).
2. Fiore, F., Massaro, E. & Barone, P. *Astr. Astrophys.* **261**, 405–414 (1992).
3. Done, C. et al. *Astrophys. J.* **400**, 138–152 (1992).
4. King, A. & Done, C. *Mon. Not. R. astr. Soc.* (in the press).
5. Abramowicz, M., Bao, G., Lanza, A. & Zhang, X.-H. *Astr. Astrophys.* **245**, 454–456 (1991).
6. Abramowicz, M. A. et al. in *The Physics of Active Galactic Nuclei* (eds Wagner, S. & Dush, W. J. 61–66 (Springer, Heidelberg, 1992).
7. Abramowicz, M., Bao, G., Karas, V. & Lanza, A. *Astr. Astrophys.* **272**, 400–406 (1993).
8. Syer, D., Clarke, C. J. & Rees, M. J. *Mon. Not. R. astr. Soc.* **250**, 505–512 (1991).
9. Sikora, M. & Begelman, M. C. *Nature* **356**, 224–225 (1992).
10. Chakrabarti, S. K. *Astrophys. J.* **411**, 610–613 (1993).
11. Clements, E. D. *Mon. Not. R. astr. Soc.* **197**, 829–834 (1981).
12. Davies, S. R. *Mon. Not. R. astr. Soc.* **244**, 93–95 (1990).
13. Davies, S. R. *Mon. Not. R. astr. Soc.* **251**, 64p–65p (1991).
14. Elvis, M., Lockman, F. J. & Wilkes, B. *Astr. J.* **97**, 777–782 (1989).
15. Patterson, J. *Astrophys. J. Suppl. Ser.* **54**, 443–493 (1984).
16. Kunieda, H. et al. *Nature* **345**, 786–788 (1990).
17. Turner, T. J., Done, C., Mushotzky, R. F., Madejski, G. M. & Kunieda, H. *Astrophys. J.* **391**, 102–110 (1992).
18. Cordova, F. in *X-ray Binaries* (eds Lewin, W. H. G., van Paradijs, J. & van der Heuvel, E. P. J.) (in the press).
19. Tennant, A., Mushotzky, R. F., Boldt, E. A. & Swank, J. H. *Astrophys. J.* **251**, 15–25 (1981).
20. Leighly, K., Kunieda, H., Tsusaka, Y., Awaki, H. & Tsuruta, S. *Astrophys. J.* (in the press).
21. Hayakawa, S. *Nature* **351**, 214–215 (1991).

22. Ishida, M. thesis, Univ. Tokyo (1991).
23. McHardy, I. in *Two Topics in X-ray Astronomy*, Proc. 23rd ESLAB Symposium (eds White, N. Hunt, J. & Battrick, B. 1111–1124 (European Space Agency, Paris, 1989).
24. Fabian, A. C. in *Frontiers of X-ray Astronomy*, (eds Tanaka, Y. & Koyama, K.) 603–610 (Universal Academy, Tokyo, 1992).
25. Rosen, S., Done, C., Watson, M. & Madejski, G. *IAU Circ. No.* 5850.

ACKNOWLEDGEMENTS. This research has been supported by NASA.

## Efficient light-emitting diodes based on polymers with high electron affinities

N. C. Greenham\*, S. C. Moratti†, D. D. C. Bradley\*, R. H. Friend\* & A. B. Holmes†

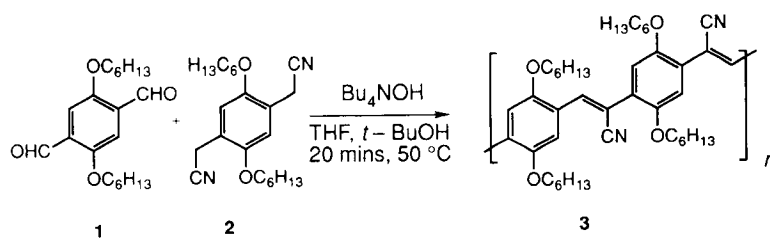
\* Cavendish Laboratory, University of Cambridge, Madingley Road, Cambridge CB3 0HE, UK

† University Chemical Laboratory, University of Cambridge, Lensfield Road, Cambridge CB2 1EW, UK

CONJUGATED polymers have been incorporated as active materials into several kinds of electronic device, such as diodes, transistors<sup>1</sup> and light-emitting diodes<sup>2</sup>. The first polymer light-emitting diodes were based on poly(*p*-phenylene vinylene) (PPV), which is robust and has a readily processible precursor polymer. Electroluminescence in this material is achieved by injection of electrons into the conduction band and holes into the valence band, which capture one another with emission of visible radiation. Efficient injection of electrons has previously required the use of metal electrodes with low work functions, primarily calcium; but this reactive metal presents problems for device stability. Here we report the fabrication of electroluminescent devices using a new family of processible poly(cyanoterephthalidene)s. As the lowest unoccupied orbitals of these polymers (from which the conduction band is formed) lie at lower energies than those of PPV, electrodes made from stable metals such as aluminium can be used for electron injection. For hole injection, we use indium tin oxide coated with a PPV layer; this helps to localize charge at the interface between the PPV and the new polymer, increasing the efficiency of recombination. In this way, we are able to achieve high internal efficiencies (photons emitted per electrons injected) of up to 4% in these devices.

Since our first report of electroluminescence in poly(*p*-phenylenevinylene), (PPV)<sup>2</sup>, a variety of conjugated polymers<sup>3–7</sup> have been shown to exhibit electroluminescence<sup>8,9</sup>. A typical polymer light-emitting diode (LED) comprises a thin film of polymer sandwiched between metal electrodes, one of which is semi-transparent. Under an applied bias, oppositely charged carriers are injected from the opposing contacts and are swept through the device by the electric field. These carriers may then capture one another within the device to form excitons, and the singlets amongst them may then decay radiatively, giving out light at a wavelength characteristic of the energy gap of the polymer. In order to achieve high electroluminescence efficiency, it is necessary to balance the rates of injection of electrons and holes from opposite contacts into the device. For the conjugated polymers investigated so far, electron injection has proved more difficult than hole injection, and it has been necessary to use metals with low work functions (such as calcium) as the electron-injecting contact in order to achieve good efficiencies<sup>3</sup>. Calcium is highly susceptible to atmospheric degradation, and is difficult to encapsulate, so it would clearly be advantageous to be able to use metals with higher work functions (such as aluminium) which possess greater stability. In the present work we have designed polymers with increased electron affinity to reduce the barrier to electron injection. Another strategy to improve device efficiency is to use additional organic charge-transporting layers between the emissive layer and one or both of the electrodes.

FIG. 1 Synthesis of the cyano-substituted polymer 3. Equimolar quantities of compounds 1 and 2 were treated with 5 mol%  $(C_4H_9)_4NOH$  in tetrahydrofuran and *t*-butanol (*t*BuOH) (1:1) at 50 °C for 20 min, and the resulting red precipitate was filtered and washed with methanol.  $^1H$  NMR: ( $CDCl_3$ , 250 MHz)  $\delta$  0.7–2.0 (22H, m), 4.09 (4H, m), 7.16 (1H, s), 7.93 (1H, s), 8.10 (1H, s), where  $\delta$  indicates proton chemical shift against tetramethylsilane as internal standard ( $\delta=0$ ), m and s indicate multiplet and singlet respectively. Gel permeation chromatography against polystyrene standards indicates a number-average molecular weight of 4,000.



The aim is to introduce energy barriers to electrons or holes at the heterojunction between the layers, and thus to confine charge carriers within the device. The confined charge at the interfaces acts to redistribute the electric field within the device so as to improve the balance of electron and hole injection. The emission is also moved away from the metal electrodes which may act as quenching sites for singlet excitons. This technique is well-established in molecular organic LEDs<sup>10,11</sup> and we have shown recently that it is possible to achieve improved efficiency in a PPV LED by incorporating an electron-transporting layer, formed as a blend of a molecular semiconductor in a polymeric matrix, between the PPV and the electron-injecting contact<sup>12,13</sup>. Other groups have demonstrated the use of hole-transporting layers with conjugated polymers<sup>14,15</sup>. We report here the use of PPV as a hole-transporting layer together with our new polymers to achieve greatly increased efficiencies.

Insoluble cyano-substituted polymers based on poly(arylenevinylene)s have been reported by several groups<sup>16,17</sup>. We have designed a family of soluble highly fluorescent poly(cyanoterephthalylidene)s in which each arylene fragment carries solubilizing long-chain alkoxy substituents. The polymer (3) was synthesized by Knoevenagel condensation polymerization of the 2,5-bis(hexyloxy)terephthalaldehyde (1) with the 2,5-bis(hexyloxy)benzene-1,4-diacetonitrile (2) as shown in Fig. 1. Careful control of reaction conditions is required to avoid Michael addition which may lead to inferior polymers.

Optical absorption and emission (photoluminescence) spectra of the polymer 3 are shown in Fig. 2. Thin films (100–300 nm)

were formed by spin-coating from chloroform solution onto glass substrates coated with indium tin oxide. Other devices were formed by spin-coating the tetrahydrothiophenium leaving-group precursor to PPV<sup>18</sup> onto the indium tin oxide substrate. The precursor was then converted to PPV by heating at 220 °C for 12 h under vacuum to give a final PPV layer of thickness in the range 100–270 nm before depositing 3. Electron-injecting contacts (area 10 mm<sup>2</sup>) of calcium, aluminium or gold were formed by vacuum evaporation. Current-voltage characteristics of the devices were measured while simultaneously measuring the light output using a calibrated silicon photodiode. Internal quantum efficiencies were calculated, taking into account refraction at the polymer-glass-air interfaces, and the electroluminescence emission spectra were measured.

Single-layer devices of polymer 3 showed uniform red emission under forward bias, with the same spectrum as the photoluminescence. Fields of  $\sim 1.2 \times 10^6$  V cm<sup>-1</sup> were required to obtain current densities of 5 mA cm<sup>-2</sup>. Similar internal quantum efficiencies, up to 0.2%, were obtained with both calcium and aluminium contacts. For other conjugated polymers, such as PPV<sup>8</sup>, at least a tenfold reduction in efficiency is found in changing the electron-injecting contact from calcium to aluminium, which has a work function of the order of 1 eV greater than that of calcium. These results indicate that electron injection is greatly improved by the introduction of cyano groups at some of the ethylidene linkages in poly(arylenevinylene)s, with the effect that device efficiency is now determined by processes at the indium tin oxide electrode.

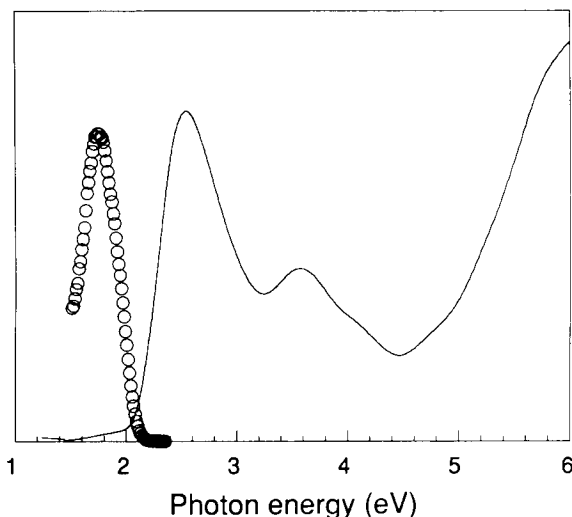


FIG. 2 Absorption (solid line) and emission (circles) spectra of a thin film of polymer 3. Emission spectra were measured under laser excitation at 457 nm, using a monochromator and photomultiplier tube whose spectral response had been calibrated using a tungsten lamp of known spectral output. The peak emission wavelength is 710 nm. (Vertical axis is in arbitrary units, linear scale.)

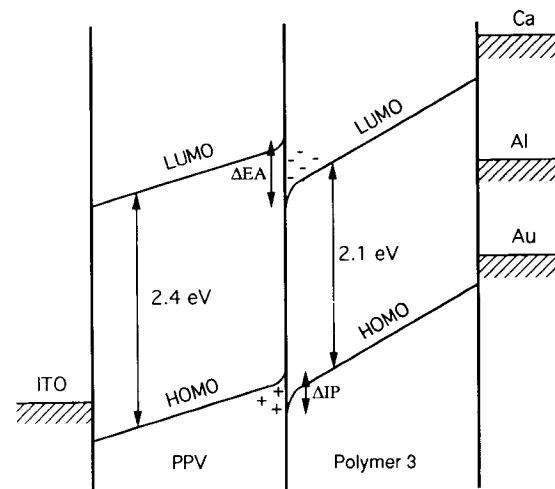


FIG. 3 Schematic energy-level diagram for a bilayer device under forward bias. The absolute energies of many of the levels are not known accurately, but the diagram shows the relative positions of the HOMO and LUMO levels in the polymers, and the Fermi levels of the various possible metal contacts. The differences in electron affinity ( $\delta EA$ ) and ionization potential ( $\delta IP$ ) between PPV and polymer 3 are shown. ITO, indium tin oxide.

Polymer bilayer devices using PPV as a hole-transporting layer also have uniform red electroluminescence. The spectrum was again similar to the photoluminescence spectrum of 3, with no evidence of emission from the PPV layer. The introduction of the PPV layer causes a significant reduction in the field (drive voltage/total polymer layer thickness) required to drive the device. A current density of  $5 \text{ mA cm}^{-2}$  requires only a field of  $\sim 4 \times 10^5 \text{ V cm}^{-1}$  with aluminium or calcium electrodes, comparable to the best of the sublimed molecular film devices<sup>10,11</sup>. Outputs of  $5.2 \text{ mW sr}^{-1} \text{ A}^{-1}$  were obtained normal to the plane of the device, giving a brightness of  $2.6 \text{ W sr}^{-1} \text{ m}^{-2}$  at a current density of  $50 \text{ mA cm}^{-2}$ . The emission was roughly lambertian over the entire forward hemisphere. This corresponds to an internal quantum efficiency of 4%. Again, comparable efficiencies were obtained with aluminium and calcium electrodes. With a gold electrode, typical efficiencies of 1% were obtained, but increased fields were required (approximately  $7 \times 10^5 \text{ V cm}^{-1}$  for  $5 \text{ mA cm}^{-2}$ ). The reduction in drive field compared with the single-layer devices indicates that charge injection is improved in the bilayer structure, and the increase in efficiency is consistent with significant charge confinement at the interface between the PPV and polymer 3 layers.

Data from differential pulse polarography on insoluble poly(cyanoterephthalylidene)s<sup>19</sup> indicates that the highest occupied molecular orbital (HOMO) and lowest unoccupied molecular orbital (LUMO) levels are lowered by 0.6 and 0.9 eV, respectively, compared with those of PPV. Preliminary cyclic voltammetry results for polymer 3 show similar trends. These offsets are large enough to present a significant barrier at the heterojunction to both electrons and holes at room temperature, leading to charge confinement. A schematic energy level diagram is shown in Fig. 3. By confining charges at the interface, a large field is established which promotes tunnelling through the barriers. We believe that emission occurs either when a hole tunnels through the barrier and forms an exciton directly in polymer 3, or when an electron tunnels into the PPV and forms an exciton which then diffuses into the lower-energy polymer 3 and decays there. Exciton generation thus takes place very close to the heterojunction, so that emission is seen only from the lower-gap polymer, which is, in this case, the cyano-substituted PPV. We consider that device efficiency, and the drive voltage required to establish the forward current, are determined primarily by the

characteristics of the polymer-polymer heterojunction rather than the two electrode-polymer contacts.

The synthetic route to polymer 3 lends itself to considerable variation. By changing the monomer units, we have prepared a range of polymers exhibiting improved electroluminescence efficiencies with a range of emission spectra. An example of an orange-yellow-emitting polymer (4) is shown in Fig. 4. This polymer gives internal quantum efficiencies of  $\sim 2\%$  when used in place of polymer 3 in bilayer structures with PPV.

The demonstration of high efficiencies in polymer LEDs using metal electrodes which are not prone to oxidation represents an important step in the development of these devices. Long-term stability, both under storage and under drive, must be demonstrated before these devices can find applications, and there is much to be learned yet about the nature of the polymer-electrode interfaces. However, promising lifetime studies have been reported for indium tin oxide-PPV-Al devices, with operation without failure to 700 h<sup>20</sup>, and recent studies of the Al-PPV interface indicate the formation of a stable covalently bonded structure<sup>21</sup>. □

Received 20 July; accepted 26 August 1993.

- Burroughes, J. H., Jones, C. A. & Friend, R. H. *Nature* **335**, 137-141 (1988).
- Burroughes, J. H. et al. *Nature* **347**, 539-541 (1990).
- Braun, D. & Heeger, A. J. *Appl. Phys. Lett.* **58**, 1982-1984 (1991).
- Ohmori, Y., Uchida, M., Muro, K. & Yoshino, K. *Jap. J. appl. Phys.* **30**, L1938-L1940 (1991).
- Ohmori, Y., Uchida, M., Muro, K. & Yoshino, K. *Jap. J. appl. Phys.* **30**, L1941-L1943 (1991).
- Grem, G., Leditzky, G., Ullrich, B. & Leising, G. *Adv. Mater.* **4**, 36-37 (1992).
- Burn, P. L. et al. *Nature* **356**, 47-49 (1992).
- Hoimes, A. B. et al. *Synth. Met.* **55-57**, 4031-4040 (1993).
- Friend, R. H., Bradley, D. D. C. & Hoimes, A. B. *Phys. World* **5**, 42-46 (1992).
- Tang, C. W. & VanSlyke, S. A. *Appl. Phys. Lett.* **51**, 913-915 (1987).
- Adachi, C., Tsutsui, T. & Saito, S. *Appl. Phys. Lett.* **57**, 531-533 (1990).
- Burn, P. L. et al. in *Electrical, Optical, and Magnetic Properties of Organic Solid State Materials* Vol. 245 (eds Chiang, L. Y., Garito, A. F. & Sandman, D. J.) 647-654 (Mater. Res. Soc. Symp. N, Pittsburgh, 1992).
- Brown, A. R. et al. *Appl. Phys. Lett.* **61**, 2793-2795 (1992).
- Ohmori, Y., Uchida, M., Muro, K. & Yoshino, K. *Solid St. Commun.* **80**, 605-608 (1991).
- Doi, S., Kuwabara, M., Noguchi, T. & Ohnishi, T. *Synth. Met.* **55-57**, 4174-4179 (1993).
- Lenz, R. W. & Handlovits, C. E. *J. org. Chem.* **25**, 813-817 (1960).
- Hörhold, H.-H. *Z. Chem.* **12**, 41-52 (1972).
- Burn, P. L. et al. *J. chem. Soc., Perkin Trans. 1*, 3225-3231 (1992).
- Helbig, M. & Hörhold, H.-H. *Makromol. Chem.* **194**, 1607-1618 (1993).
- Karg, S. et al. in *Proc. 6th Symp. on Unconventional Photoactive Solids* Leuven, Belgium, 1993; also as *Molec. Cryst. liq. Cryst.* (in the press).
- Dannetun, P. et al. *Synth. Met.* **55-57**, 212-217 (1993).

ACKNOWLEDGEMENTS. We thank the SERC, Cambridge Display Technology and the Nuffield Foundation (R.H.F.) for financial support. We acknowledge assistance from P. J. Hamer and D. R. Baigent, and from E. C. Constable and A. Cargill-Thompson.

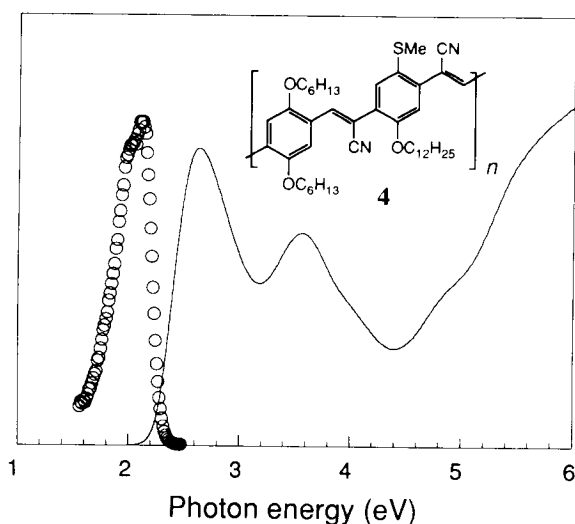


FIG. 4 Absorption (solid line) and emission (circles) spectra and structure of polymer 4, measured under the same conditions as for Fig. 2. The peak emission wavelength is 610 nm. (Vertical axis is in arbitrary units, linear scale.)

## Prebiotic ammonia from reduction of nitrite by iron (II) on the early Earth

David P. Summers & Sherwood Chang

NASA-Ames Research Center, Moffett Field, California 94035, USA

THEORIES for the origin of life require the availability of reduced (or 'fixed') nitrogen-containing compounds, in particular ammonia. In reducing atmospheres, such compounds are readily formed by electrical discharges<sup>1,2</sup>, but geochemical evidence suggests that the early Earth had a non-reducing atmosphere<sup>1,3-6</sup>, in which discharges would have instead produced NO (refs 7-10). This would have been converted into nitric and nitrous acids and delivered to the early oceans as acid rain<sup>11</sup>. It is known<sup>12-15</sup>, however, that Fe(II) was present in the early oceans at much higher concentrations than are found today, and thus the oxidation of Fe(II) to Fe(III) provides a possible means for reducing nitrites and nitrates to ammonia. Here we explore this possibility in a series of experiments which mimic a broad range of prebiotic seawater conditions (the actual conditions on the early Earth remain poorly constrained). We find